Sensing - Magnetic Compass with Tilt Compensation

AN2272

Author: Vadym Grygorenko
Associated Project: Yes
Associated Part Family: CY8C27xxx, CY8C29xxx
Software Version: PSoC Designer™ 5.1(SP1.1)
Associated Application Notes: None

Application Note Abstract

AN2272 presents a low-cost, digital 3-axis magnetic compass based on the Honeywell HMC1043 Magneto Resistive Sensor. A dual-axis accelerometer is used to provide tilt sensing for heading correction. Several full-featured and simplified design versions are also described.

Introduction

This design implements a 3-axis, magneto resistive sensor-based digital compass with tilt compensation. Minimal external components are used, which allows for low-cost and compact implementation.

Main features of the presented design include:

- High precision and resolution up to 0.25 degrees.
- Wide range tilts compensation.
- Procedures to store calibration data in the internal EEPROM.
- Ability to transmit data to a PC via RS-232 interface for debug and other purposes.

Magnetic Compass Background

All electronic compasses are based on the measurements of the Earth's magnetic field. The Earth can be considered a magnetic dipole with poles located near the geographic North Pole and South Pole (see Figure 1).

Figure 1. Earth's Magnetic Field

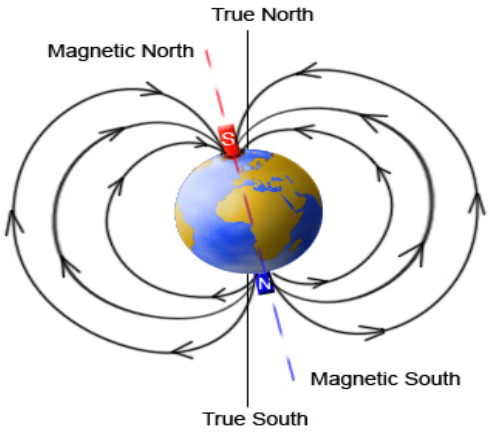

It is easy to observe that the magnetic field vector is parallel to the surface near the equator. In the Northern Hemisphere, that vector points down toward the North Pole, as shown in Figure 2.

Figure 2. Magnetic Field Inclination Angle

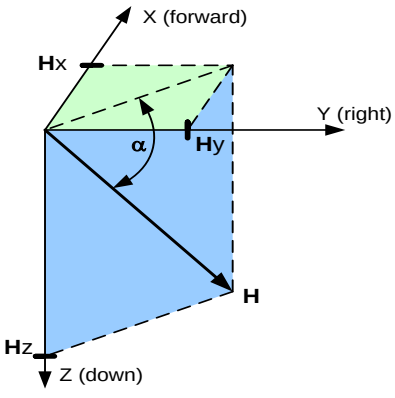

The angle between the magnetic vector and the horizontal plane, XY, is called the dip or inclination angle (α in Figure 2). This angle is mainly dependent on the geographical latitude (see Figure 3).

Figure 3. Magnetic Vector Inclination Angle Map From www.ngdc.noaa.gov

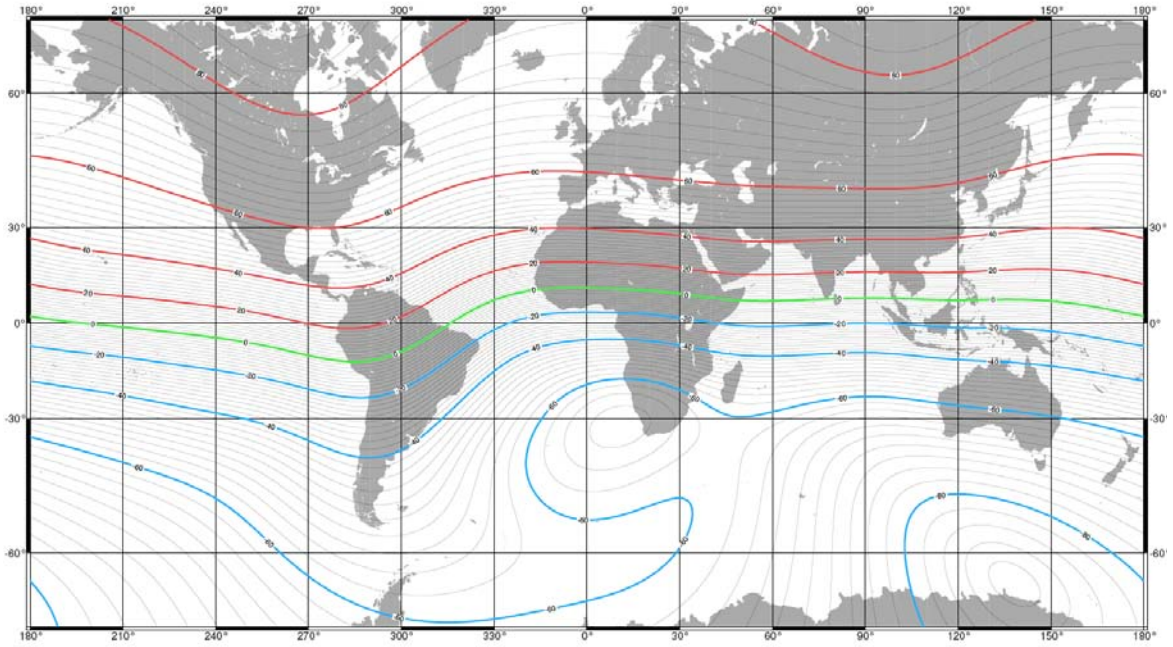

A common approach used to estimate the heading is to measure two orthogonal components of the magnetic vector (H_x and H_y according to Figure 2) and calculate the heading as the arctangent of their ratio:

$$Heading = \arctan\left(\frac{H_y}{H_x}\right) \qquad \text{Equation 1}$$

This equation is correct only when the magnetic sensor is precisely leveled. If some tilt is present, the measured values H_x and H_y change and the resultant heading is not exact.

This error is enhanced by the vertical component of the magnetic vector. For instance, if the inclination angle is about 60 degrees and the compass is tilted at 5 degrees to level, the azimuth measurement error will be up to 8 degrees.

To avoid tilt error, a 3-axis magnetic sensor with an additional tilt measurement circuit can be used. A 3-axis sensor provides the Earth's magnetic vector coordinates relative to a compass local coordinate frame. These values are not enough to calculate the true heading. Additional information about the compass space orientation is necessary.

This information is obtained from the tilt sensor, similar to an accelerometer. If the compass is not accelerating, the tilt sensor measures the angles between the compass and the gravity vector. Based on the tilt sensor values, the locally measured vector coordinates H_x, H_x and H_z are converted to a reference coordinate and the heading is calculated according to Equation (1).

The presented design uses a Honeywell magneto resistive sensor, HMC1043, for H_x, H_x and H_z measurement and an Analog Devices dual-axis accelerometer, ADXL322, as a tilt sensor.

Device Design Basis

Allow us to consider a few geometric aspects of the vector measurements on the tilted platform. Assume the coordinate system is chosen in such a way that the X-axis is oriented forward, the Y-axis is to the right, and the Z-axis is downward (Figure 4). The stationary coordinate frame will be signed as XYZ and the local tilted coordinate system is X'Y'Z'.

Figure 4. Pitch and Roll Description

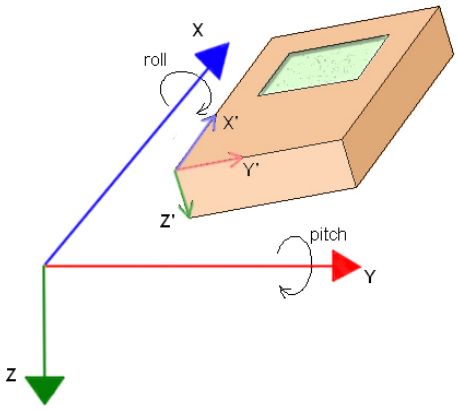

There are several ways to describe rotation of the coordinate frame of the compass relative to the fixed frame, such as quaternion, Euler angles, roll-pitch-heading, rotation matrix, spin matrix and so on. The aircraft convention of the rotation angles is used below. Roll angle (θ) is defined as rotation around the X-axis. Pitch angle (ϕ) is defined as rotation around the Y-axis. All rotations are performed counter-clockwise, if viewed from the positive axis direction toward the origin of the coordinate frame. The X-axis and Y-axis rotation sequence is important (try to rotate an object 90 degrees around the X-axis and then around the Y-axis, or in the reverse order, and the results will be different).

Therefore, the assumed rotation to be performed is around the X-axis first, then around the Y-axis (roll, then pitch).

Each basic rotation can be described by the rotation matrix that transforms the coordinates from the stationary coordinate frame of XYZ to the rotated tilted coordinate system of X'Y'Z'. The roll rotation matrix is:

$$C_r = \begin{pmatrix} 1 & 0 & 0 \\ 0 & \cos\theta & \sin\theta \\ 0 & -\sin\theta & \cos\theta \end{pmatrix} \quad \text{Equation 2}$$

The pitch rotation matrix is:

$$C_p = \begin{pmatrix} \cos\theta & 0 & -\sin\theta \\ 0 & 1 & 0 \\ \sin\phi & 0 & \cos\phi \end{pmatrix} \quad \text{Equation 3}$$

Rotation transformation of the coordinates occurs using either of the following equations:

$$\begin{pmatrix} x' \\ y' \\ z' \end{pmatrix} = C_r \cdot C_p \cdot \begin{pmatrix} x \\ y \\ z \end{pmatrix} \quad \text{Equation 4}$$

$$\begin{pmatrix} x' \\ y' \\ z' \end{pmatrix} = \begin{pmatrix} \cos\phi & 0 & -\sin\phi \\ \sin\theta\sin\phi & \cos\theta & \sin\theta\cos\phi \\ \cos\theta\sin\phi & -\sin\theta & \cos\theta\cos\phi \end{pmatrix} \cdot \begin{pmatrix} x \\ y \\ z \end{pmatrix} \quad \text{Equation 5}$$

The magnetic sensor measures the $x'y'z'$ components of the Earth's magnetic vector. For azimuth estimation, these values should be converted to the stationary coordinate system. That conversion is performed using an inverted rotation matrix:

$$\begin{pmatrix} x \\ y \\ z \end{pmatrix} = \begin{pmatrix} \cos\phi & \sin\theta\sin\phi & \cos\theta\sin\phi \\ 0 & \cos\theta & -\sin\theta \\ -\sin\phi & \sin\theta\cos\phi & \cos\theta\cos\phi \end{pmatrix} \cdot \begin{pmatrix} x' \\ y' \\ z' \end{pmatrix} \quad \text{Equation 6}$$

Since the *z* coordinate is not used for azimuth estimation, the tilt-compensated values for x and y can be evaluated as:

$$x = x'\cos\phi + y'\sin\theta\sin\phi + z'\cos\theta\sin\phi \quad \text{Equation 7}$$

$$y = y'\cos\theta - z'\sin\theta \quad \text{Equation 8}$$

x' and y' are the measured components of the magnetic vector.

Consequently, to convert the measured values into tilt-compensated values, the roll and pitch angles should be estimated. This task is solved by a dual-axis accelerometer.

The accelerometer output signals are proportional to the gravitation vector projections on the X'Y' plane (see Figure 5).

Figure 5. Gravitation Vector Projections

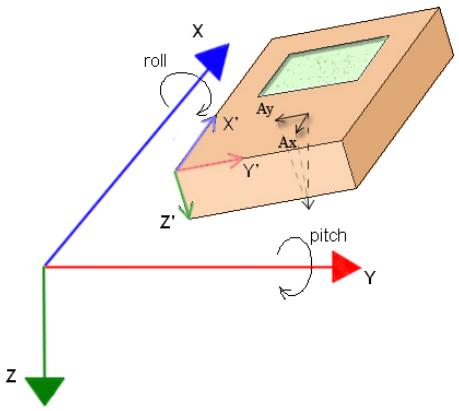

The accelerometer output values can be considered as the sin of the angle between the X'-axis and the level Ax, and between the Y'-axis and the level Ay. Sometimes these angles are called the pitch angle P and the roll angle R. However, these angles should not be confused with the θ and ϕ angles that were previously defined.

Nevertheless, in most application notes devoted to tilt compensation, including *AN00022 Electronic Compass Design using KMZ51 and KMZ52* by Philips (see Figure 24, Definition of Pitch and Roll, on p.32); these angles are directly substituted in the corresponding values shown in Equation 7 and Equation 8.

$$A_x = -\sin\phi \quad \text{Equation 9}$$

$$A_y = \sin\theta \qquad \text{Equation 10}$$

This assumption is valid only when the tilt is small. Allow us to consider this issue in more detail. The normalized accelerometer outputs Ax and Ay can be considered transformed by the rotation matrix in Equation (5) of the normalized gravitation vector:

$$\begin{pmatrix} A_x \\ A_y \\ A_z \end{pmatrix} = \begin{pmatrix} \cos\phi & 0 & -\sin\phi \\ \sin\theta\sin\phi & \cos\theta & \sin\theta\cos\phi \\ \cos\theta\sin\phi & -\sin\theta & \cos\theta\cos\phi \end{pmatrix} \cdot \begin{pmatrix} 0 \\ 0 \\ 1 \end{pmatrix} \qquad \text{Equation 11}$$

Thus,

$$A_x = -\sin\phi \qquad \text{Equation 12}$$

$$A_y = \sin\theta\cos\phi \qquad \text{Equation 13}$$

It is easy to observe from Equations 12 and 13 that, in the case of a small pitch angle ϕ, when $\cos\phi \approx 1$ a commonly used simplification of the roll is, the pitch angle's estimation is acceptable. Therefore, if the wide range tilt compensation is required, then Equations 12 and 13 should be used.

Using Equations 12 and 13 and standard trigonometry identities, the values for the tilt compensation formula, Equations 7 and 8, can be given as:

$$\sin\phi = -A_x \qquad \text{Equation 14}$$

$$\cos\phi = \sqrt{1-\sin^2\phi} = \sqrt{1-A_x^2} \qquad \text{Equation 15}$$

$$\sin\theta = -\frac{A_y}{\cos\phi} = \frac{A_y}{\sqrt{1-A_x^2}} \qquad \text{Equation 16}$$

$$\cos\theta = \sqrt{1-\sin^2\theta} = \sqrt{\frac{1-A_x^2-A_y^2}{1-A_x^2}} \qquad \text{Equation 17}$$

Since, for navigation purposes only, the ratio of the measured values is important (see Equation 1), both Equations 7 and 8 can be multiplied by the same value. It is convenient to multiply these equations by $\cos\phi$ to avoid dividing operations during microcontroller implementation.

Finally, the equations for the tilt compensation are next:

$$x = x'\left(1-A_x^2\right) - y'A_xA_y - z'A_x\sqrt{1-A_x^2-A_y^2} \qquad \text{Equation 18}$$

$$y = y'\sqrt{1-A_x^2-A_y^2} - z'A_y \qquad \text{Equation 19}$$

x', y' and z' are the measured values of the magnetic vector, and A_x and A_y are the normalized measurements of the accelerometer.

$$Heading = \arctan\frac{y}{x} \qquad \text{Equation 20}$$

To calculate the geographic azimuth as a clockwise angle between the north direction and X-axis, the signs of y and x must be taken into account:

$$Azimuth = \begin{cases} 180 - \arctan y/x, & x < 0 \\ -\arctan y/x, & x > 0, y < 0 \\ 360 - \arctan y/x, & x > 0, y > 0 \\ 90, & x = 0, y < 0 \\ 270, & x = 0, y > 0 \end{cases} \qquad \text{Equation 21}$$

Expressions in equations (18), (19) and (21) are used in the present design to estimate tilt compensated heading.

PSoC Implementation

The main parts of the presented design are:

- PSoC® CPU (CY8C27xxx device family).
- 3-axis magnetoresistive sensor (Honeywell HMC1043).
- Dual-axis accelerometer (Analog Devices ADXL 322).
- Sensor's signal conditioning circuit (operational amplifier).
- Magnetic sensor set/reset circuit.
- Multichannel RS-232 Driver (MAX232).
- LCD.

The simplified hardware architecture is presented in Figure 6.

Figure 6. Compass Hardware Architecture

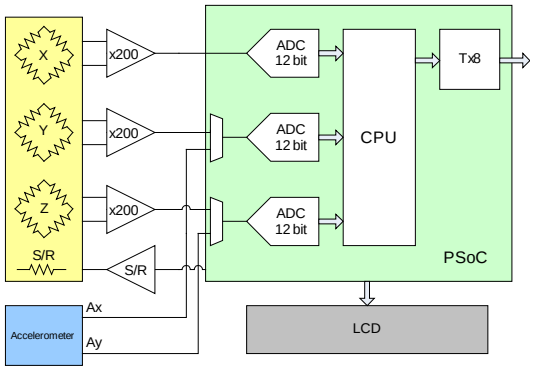

Each channel of the magneto resistive sensor is a Wheatstone bridge, which converts the magnetic field into a differential output voltage. The typical sensor sensitivity is 5 mV/gauss (at Vdd=5V). The Earth's magnetic field can reach ±800 mgauss; therefore, the useful sensor output voltage can be up to ±4 mV. The magnetic sensor also has a considerable DC offset voltage of up to ±6.25 mV. The total output signal will be up to ±10.25 mV. After an amplifier with a gain equal to 200, the amplitude is about 4 volts. This value fits in the range of an ADC with a reference of Vdd/2 ± Vdd/2.

The output of the accelerometer and the magnetic sensor is ratio metric. The output signal peak-to-peak amplitude is about 600 mV (300 mV/g). With a 12-bit ADC tilt measurement, the error will be no more than 0.5 percent, without additional amplification.

An important advantage of implementing the PSoC device inside the compass is the option to use a three-channel ADC. This allows simultaneous conversion of all magnetoresistive sensor output signals (X, Y and Z) or accelerometers signals. Traditional methods use one ADC to sequentially convert all inputs. If the device is moved, then the measurements will reflect vector components at different moments, which can cause additional errors. The present device measures all of the values simultaneously, thus improving the accuracy of the results. The ADC conversion time is set to about 60 ms, which allows about 7 azimuth measurements per second to be received. This value can easily be changed, if another measurement speed is required.

The set/reset (S/R) circuit is used to compensate both the magneto resistive sensor offset and the amplifier-ADC circuit's offset.

The idea of such offset compensation is based on the option to flip the sensor's bridge output polarity using sequential high-current pulses of the opposite polarity across the S/R strap. Polarity changes in the signal are only caused by the magnetic field. The offset of the bridge and signal conditioning circuits remains unchanged. Consequently, the offset can be canceled by subtraction of the two measurements:

Reset: $Code_R = K\left(-V_{Magnetic} + V_{Offset}\right)$ Equation 22

Set: $Code_S = K\left(V_{Magnetic} + V_{Offset}\right)$ Equation 23

$$V_{Offset} = \frac{Code_R + Code_S}{2K}$$ Equation 24

$$V_{Magnetic} = \frac{Code_S - Code_R}{2K}$$ Equation 25

$Code_R$ is the ADC code after the reset pulse, $Code_S$ is the ADC code after the set pulse, V_{Offset} is the summary offset, and $V_{Magnetic}$ is the signal.

For high-precision measurements, S/R pulses can be used for each sample. But for common tasks, occasionally recalculating the offset and subtracting it from each sample is sufficient. This design recalculates V_{Offset} each 256 measurements or about twice per minute. S/R pulses are formed by the charge/dump current of the capacitor connected in serial with the S/R strap. Due to low strap resistance (about 5 Ω) the peak current reaches up to 1A which is enough to flip magnetic orientation of the sensor. The pulse width is defined by the CR time constant. It is relatively small at several microseconds. The low value of the S/R pulse's duty factor gives a small averaged power consumption of the S/R circuit in spite of the considerable peak current. Pulse energy is given by:

$$E = \frac{U^2 C}{2} = \frac{5^2 \cdot 0.5 \cdot 10^{-6}}{2} \approx 6 \text{ micro-Joules}$$ Equation 26

Taking into account the pulse's duty factor we can estimate the S/R circuit power consumption to be less than one microwatt.

Additional details on S/R operations are described in the sensor manufacturer's application notes such as Honeywell's *AN213 Set/Reset Function for Magnetic Sensors*.

The full device schematic is shown in Figure 14 in Appendix A.

Input signals from sensor are amplified by differential amplifiers U2A-U2C. Resistors for these amplifiers should be chosen with tolerance of 0.1% to avoid significant DC offset at output. It is not obligatory to use precision operational amplifier. It can be low-cost but low-noise with offset voltage no more than 1-2 mV.

Magneto resistive sensor's outputs are shunted by 1uF capacitors C9, C14 and C21. These capacitors interact with sensor output impedance of 1 kilohm and limit sensors bandwidth to about 160 Hz. Such bandwidth limitation is advisable because sensor can produce signals up to 5 MHz that can cause disturbances. The side effect of bandwidth limit is increasing of transient time after Set/Reset pulses applying. This problem is solved by software applying delay during Set/Reset operations.

All next signal processing is performed by PSoC.

Software Description

The software's main task is to perform calculations of the heading according to Equations 18, 19, and 21. These calculations are complicated by arctangent and square root functions. If a PC performs the calculations, there is no problem in using the floating-point arithmetic and standard libraries. However, in most cases, the usage of a floating point with microcontrollers is not acceptable. That is why all of the calculations in this design are performed with integer numbers. Arctangent and square root are calculated using COordinate Rotation DIgital Computer (CORDIC) algorithms that only require addition and shift operations. There are many CORDIC descriptions on the web, for instance "CORDIC FAQ." The algorithms described below are based on "Arctan(x) using CORDIC," "Square-root based on CORDIC" and sci.math.num-analysis newsgroup archives.

Allow us to consider arctangent calculations in more detail. The function $\arctan\frac{y}{x}$ denotes the angle between X-axis and vector (x;y). To estimate this angle, several rotations of the vector by predefined angles are performed. Rotations are made until the resulting vector sufficiently approaches the X-axis. The sum of these rotation angles yields the desired arctangent. The predefined angles are chosen to be $\pm\arctan\left(\frac{1}{2^n}\right)$.

The vector rotation by angle α changes its coordinates according to the rotation transformation:

$$x' = x\cos\alpha - y\sin\alpha \quad \text{Equation 27}$$

$$y' = x\sin\alpha + y\cos\alpha \quad \text{Equation 28}$$

Or,

$$x' = \cos\alpha\left[x - \tan\alpha\right] \quad \text{Equation 29}$$

$$y' = \cos\alpha\left[x\tan\alpha + y\right] \quad \text{Equation 30}$$

For angle estimation (if vector length is insignificant), the term $\cos\alpha$ can be ignored. If $\tan\alpha_i = \pm\frac{1}{2^i}$, then

$$x_{i+1} = x_i - \frac{y_i \cdot d_i}{2^i} \quad \text{Equation 31}$$

$$y_{i+1} = y_i - \frac{x_i \cdot d_i}{2^i} \quad \text{Equation 32}$$

$d_i = \pm 1$. The angles α_i are calculated at design time and stored in a look-up table. The sum of each rotation angle is stored in the angle accumulator:

$$Ang_{i+1} = Ang_i + d_i \cdot \alpha_i \quad \text{Equation 33}$$

Each following rotation direction is determined in such a way to approach the resulting vector toward the X-axis:

$d_i = -1$ **if** $y_i > 0$ **, +1 otherwise** Equation 34

Iterations in Equations 31, 32, 33, and 34 are performed until $\alpha_i < 1$. This procedure is shown in a simplified flowchart in Figure 7.

To achieve precision better than 1°, the weight of the least significant bit (LSB) of the angle accumulator Ang should be less than 1°. In the present design, it is assumed that 1 LSB = 0.25° or $360° \rightarrow \text{Ang} = 360 \cdot 4$. The described algorithm is implemented in the **ArcTan2 ()** function.

Another extension of the CORDIC algorithm is used to calculate the square root function in Equations 18 and 19. The main idea of this algorithm is to determine whether or not a square of each binary digit is present in the input value.

If $s = \sqrt{a}$ and s contains binary 1 with weight 2^i, then a contains 2^{2i}. In that way, the iterative algorithm can be written as:

$$s_{21} = 2^{i+1} \cdot s + 2^{2i}; \quad \text{Equation 35}$$

if $a \geq s_{21}$, **then** $s+ = 2^i; a- = s_{21}$ Equation 36

Iterations start at $i = 8$; $s = 0$ and they are performed until $i = 0$ (see Figure 8). It is easy to observe that this procedure requires only addition and shift operations; therefore, it is friendly to microcontroller implementation. The described algorithm is implemented in the function **ISqrt()**.

Figure 7. Simplified Flowchart of ArcTan2 Function

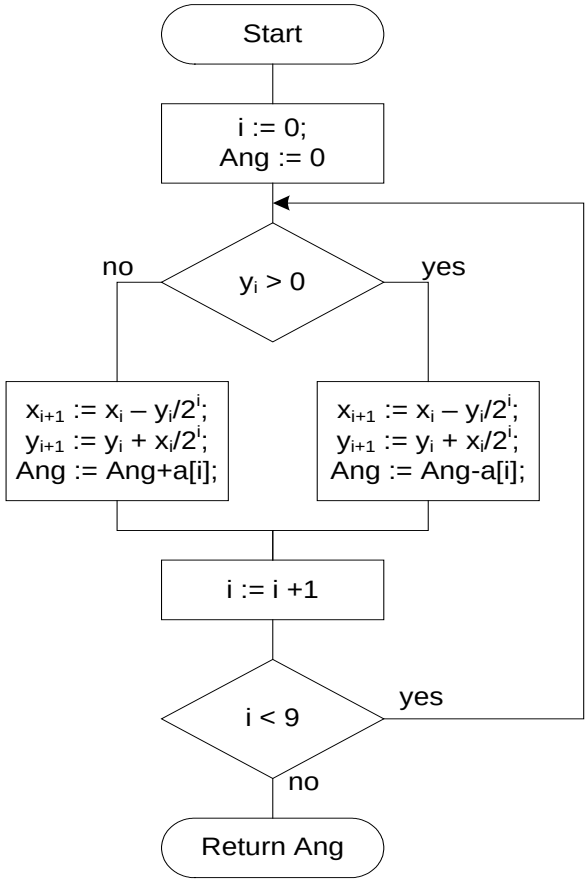

Figure 8. Flowchart of ISqrt Function

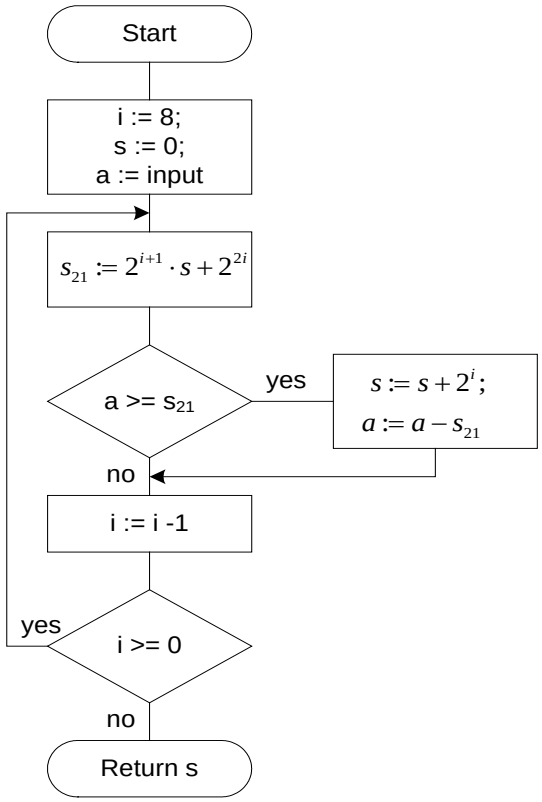

The measured values of the magnetic vectors x', y' and z', before substitution into equations (18) and (19), are filtered by a low-pass second order digital IIR-filter as described by this equation:

$$f_n = \frac{1}{4}(c_n + 2 \cdot c_{n-1} + c_{n-2}) + f_{n-1} - \frac{1}{4} f_{n-2} \qquad \text{Equation 37}$$

c_n is the samples of input values and f_n is the filter output.

This filter has a gain of 4 and cut-off frequency at approximately 0.07 times the sample rate. The presented design samples data at a rate of about 7 Hz; therefore, the cut-off frequency is close to 0.5 Hz. The described filtration is implemented in the procedures **FiltrA()**, **FiltrB()** and **FiltrC()** for x', y' and z', correspondingly.

There are several additional functions in the firmware. The complete list and brief description is shown in Table 1.

Table 1. Functions Description

Function Name	Description
Main	Performs startup device configuration, measures magnetic vector and tilt, calculates azimuth.
FiltrA, FiltrB, FiltrC	Low-pass digital filters for measured magnetic vector components.
ArcTan2	Calculates ArcTan(y/x) taking into account signs of y and x.
ISqrt	Calculates square root.
Delay	Makes n x 15 ms delay using low-precision sleep timer.
DoSetReset	Forms S/R pulse's sequence for magnetic sensor, calculates offsets.
DoCalibrM	Performs hard iron offset and axis scale factor calibration.
DoCalibrA	Calibrates accelerometer.
DoCalibrD	Performs true north calibration.
SaveDefaults	Saves calibration results into internal EEPROM as power-on defaults.

Compass Calibration

There are many known compass error factors that are described in detail in a number of papers. For instance, "Applications of Magnetic Sensors for Low Cost Compass Systems." The present design implements hard iron error and true north declination angle compensation, in addition to the tilt compensation previously described.

If the compass is rotated in the horizontal plane and no disturbances are present, then the output values plot y versus x should form an ideal circle centered at the coordinate system origin. However, the real plot differs from the ideal case. The circle becomes an ellipse with the center shifted from the zero point (see Figure 9).

To compensate for the described error, the scale factors should be applied and the offset subtracted.

$$x_h = x \cdot X_{sf} - X_{off} \qquad \text{Equation 38}$$

$$y_h = y \cdot Y_{sf} - Y_{off} \qquad \text{Equation 39}$$

The scale factors X_{sf} and Y_{sf} as well as offsets X_{off} and Y_{off} are determined during the calibration procedure.

During calibration, the compass is rotated in the horizontal plane and the minimum and maximum measured values for both the X- and Y-axis are collected. Then the desired values are calculated as follows:

$$X_{sf} = \max\left(\frac{y_{\max} - y_{\min}}{x_{\max} - x_{\min}}, 1\right) \quad \text{Equation 40}$$

$$Y_{sf} = \max\left(\frac{x_{\max} - x_{\min}}{y_{\max} - y_{\min}}, 1\right) \quad \text{Equation 41}$$

$$X_{off} = \frac{x_{\max} + x_{\min}}{2} \cdot X_{sf} \quad \text{Equation 42}$$

$$Y_{off} = \frac{y_{\max} + y_{\min}}{2} \cdot X_{sf} \quad \text{Equation 43}$$

The calibration procedure is initiated by pressing the switch SW1. Then, several slow rotations in the horizontal plane are performed. To alert the device that the rotations are complete, the switch SW1 should be pressed once again. During this calibration, the compass should be exactly leveled.

The result of the applied compensation is shown in Figure 10. The attentive observer may notice that the data jitter shown in Figure 10 is a little larger than in Figure 9. That is because in Figure 10, the tilt compensation is applied along with the hard iron compensation. The tilt compensation is based on the accelerometer measurements. If the platform rotation is not steady, then the accelerometer will respond to jerks, thus introducing additional errors to measurement.

Figure 9. Real Data Plot with Magnetic Disturbances

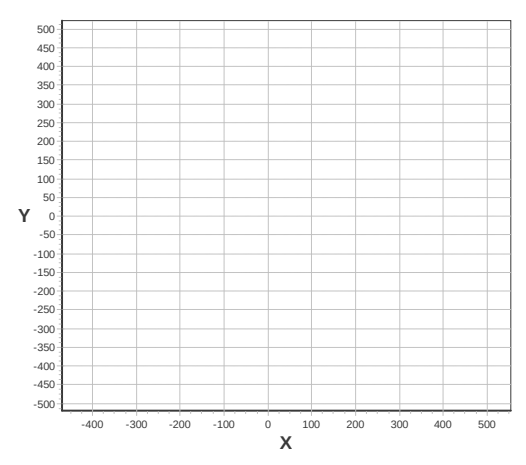

Figure 10. Real Data Plot with Applied Compensation

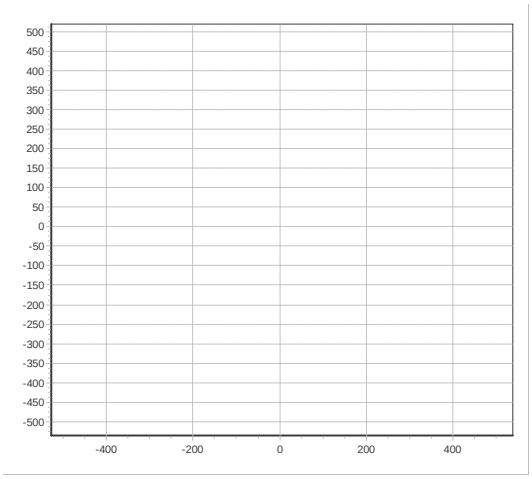

The second calibration procedure deals with the accelerometer. It measures the minimum and maximum output values for both axes when the device is directed vertically. These values are used for calculating normalized A_x, A_y values for equations (18) and (19).

Such calibration is necessary because of the variation in sensor parameters. The calibration procedure is initiated by pressing the switch SW2. Then, the device should be slowly turned vertically and rotated in the vertical plane. In other words, the device's X-axis and Y-axis should be alternately directed upward and downward. After that, the device should be placed horizontally and the switch SW2 should be pressed again, alerting the device that the procedure has ended.

The third calibration procedure compensates the difference between the geographical north direction and magnetic north. That difference is known as the declination angle. To compensate this angle, position the device so that the X-axis points in the geographical north direction, then press switch SW3. After that, the declination angle is subtracted from each measured azimuth.

All calibration results are stored in the internal EEPROM and loaded each time the device is powered-on.

Testing Results

The compass prototype was designed to verify the described algorithms. The test board is shown in Figure 11.

Figure 11. Compass Test Board

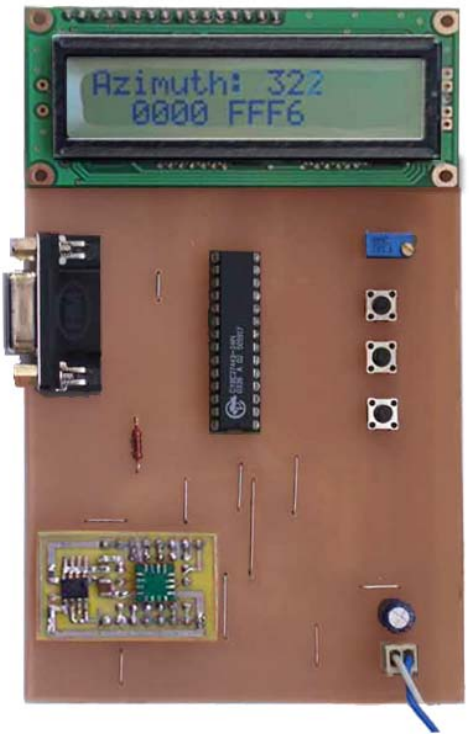

The magnetic sensor is mounted on a separate plate to facilitate mounting/unmounting operations without special equipment.

The results of the measurements are displayed on the LCD. The azimuth is displayed in the first row and the Ax and Ay hexadecimal values are displayed in the second row. The measured values are also transmitted to the PC via the RS-232 interface.

Tests were performed indoors not far from the computer and near other high-disturbance sources. The results were encouraging: the angle jitter was about ±0.25 degrees. The absolute error was not measured because of the absence of a reference compass. For comparison, similar measurements were implemented using a single ADC and a three-channel ADC. When using a single ADC, some bursts were observed and full peak-to-peak jitter reached about 3 degrees. This result proves the advantages of employing the three-channel ADC.

Simplified Compass Versions

The previously described compass implementation is appropriate for high-precision measurement systems. It is possible to simplify that design, if the precision requirements are not as strict.

For instance, the internal PSoC instrumental amplifiers can be used instead of an external opamp. Due to the limited quantity of analog blocks, only two amplifiers are available. Therefore, inputs should be multiplexed allowing alternate measurements of X, Y, Z and Ax, Ay values (see Figure 12). In this case, a dual ADC is used, instead of triple. The full device schematic is shown in Figure 15 of Appendix A.

Figure 12. Simplified Hardware Architecture for Tilt-Compensated Compass

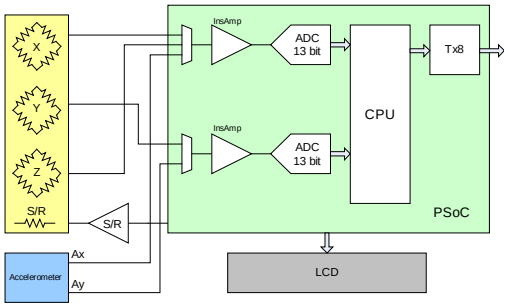

If tilt compensation is not required, then the device schematic can be simplified (see Figure 13). Internal PSoC instrumental amplifiers can be used instead of an external opamp. ADC resolution is increased to 13 bits due to the gain limit of the internal instrumental amplifiers. Measurement results are displayed on the LCD.

Figure 13. Hardware Architecture for Dual-Axis Compass

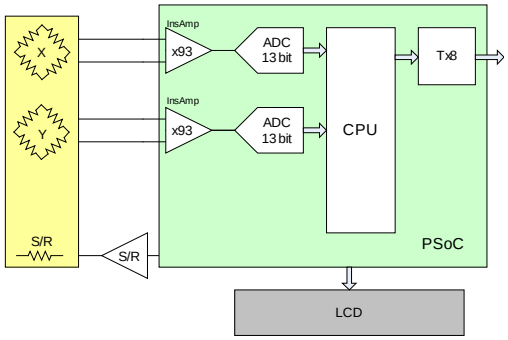

The full device schematic is shown in Figure 16 of Appendix A. There are several external components on this schematic, including the optional RS-232 interface.

Another possible design simplification can be achieved be replacing the LCD with several LEDs. These LEDs are placed counterclockwise on the circle. A lit LED indicates north. This version schematic is shown in Figure 17.

Appendix A. Device Schematics

Figure 14. Tilt-Compensated Compass Schematic

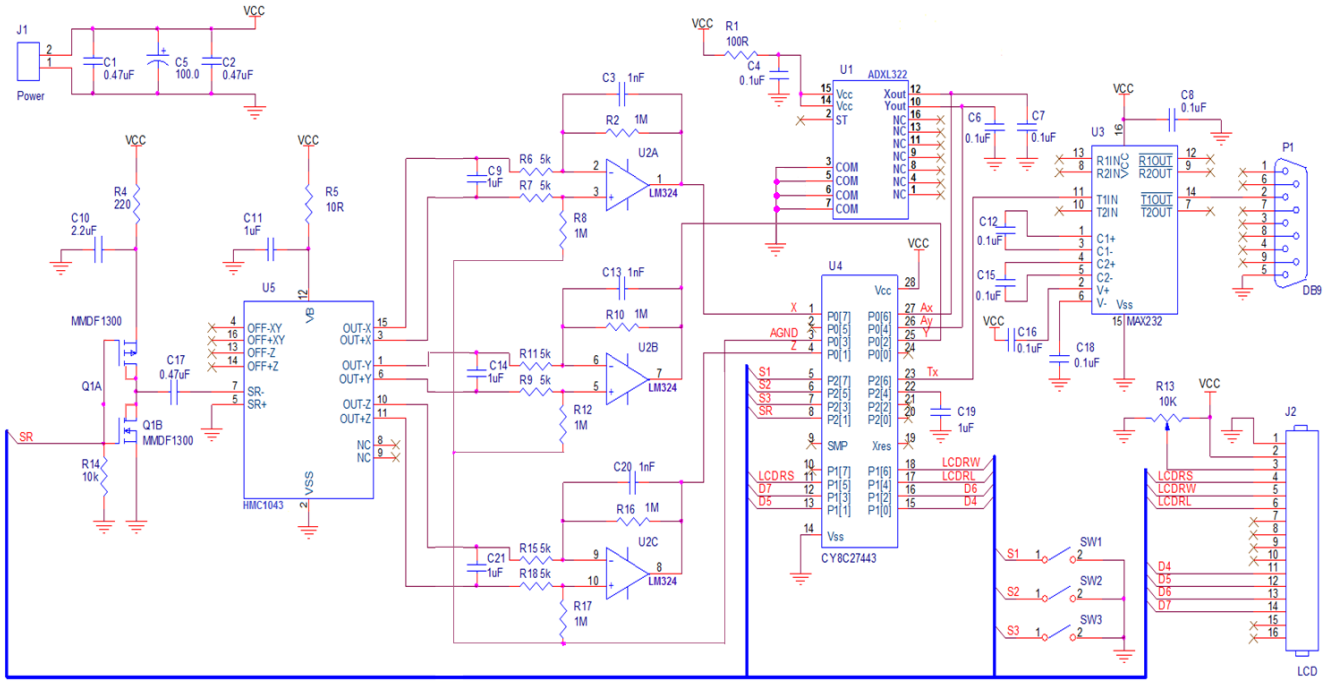

Figure 15. Simplified Tilt-Compensated Compass Schematic

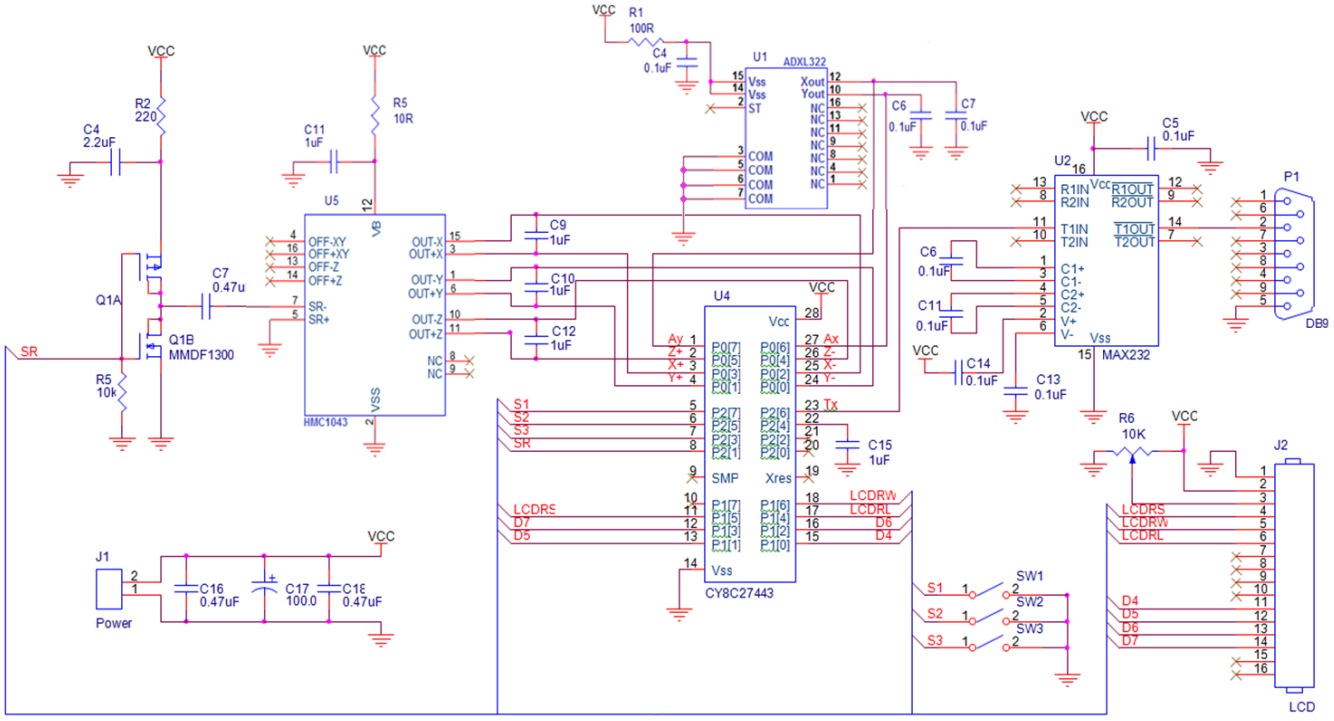

Figure 16. Dual-Axis Compass Schematic

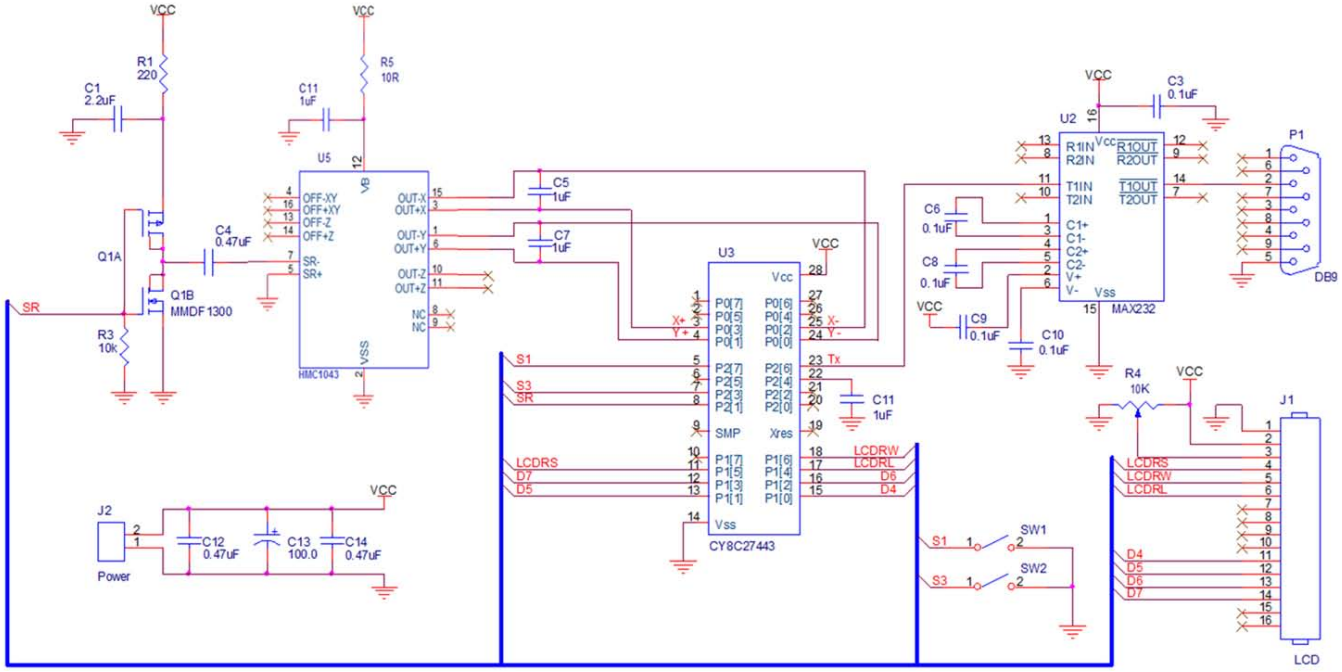

Figure 17. Simplified Compass Schematic

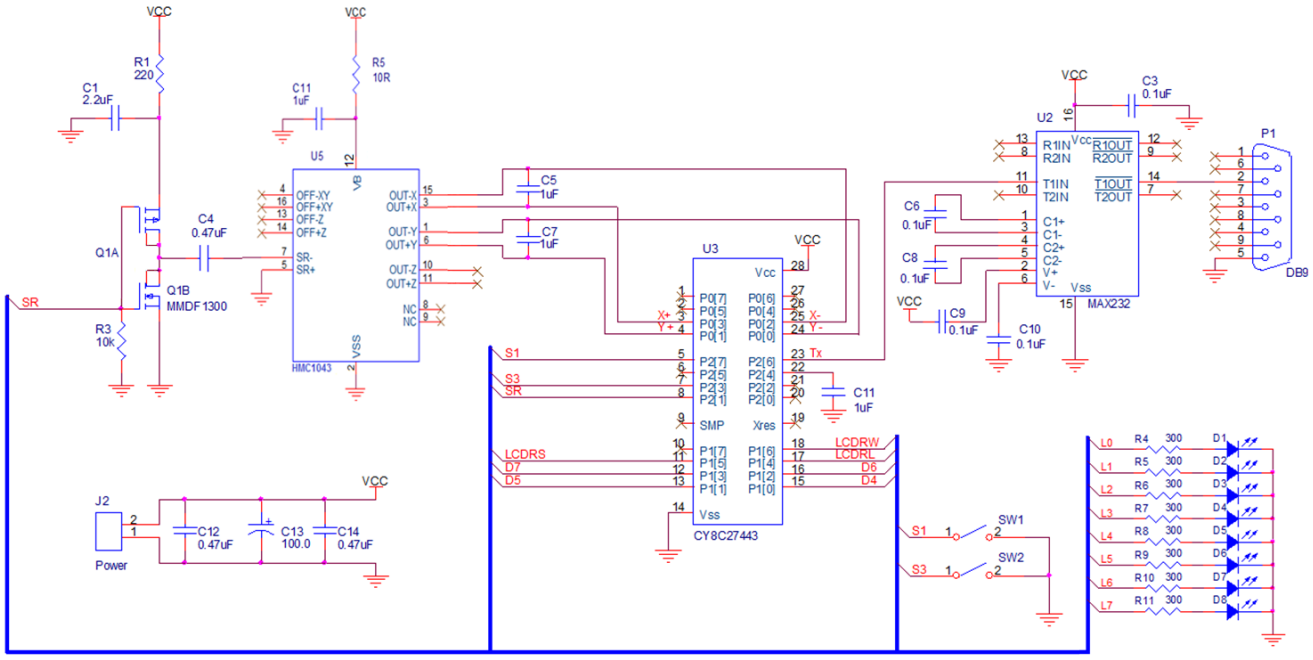

About the Author

Name: Vadym Grygorenko
Title: Sr. Application Engineer
Background: Vadym earned a radiophysics diploma in 1986 from Ivan Franko National Lviv University and his PhD in 1992. His interests include embedded systems design and application programming.
Contact: vadg_ukr@cypress.com

Document History

Document Title: Sensing - Magnetic Compass with Tilt Compensation

Document Number: 001-32379

Revision	ECN	Orig. of Change	Submission Date	Description of Change
**	1491203	YARD	10/08/2007	New Application note
*A	3283671	YARD	06/15/2011	Associated Project files zipped with source document. No changes in the document and formatted as per template. Document History details added.

In March of 2007, Cypress recataloged all of its Application Notes using a new documentation number and revision code. This new documentation number and revision code (001-xxxxx, beginning with rev. **), located in the footer of the document, will be used in all subsequent revisions.

Cypress Semiconductor
198 Champion Court
San Jose, CA 95134-1709
Phone: 408-943-2600
Fax: 408-943-4730
http://www.cypress.com/